

# Qualitative vision-based navigation based on sloped funnel lane concept

Mohamad Mahdi Kassir, Maziar Palhang, Mohammad Reza Ahamadzadeh

**Abstract**—A new visual navigation based on visual teach and repeat technique is described in this paper. In this kind of navigation, a robot is controlled to follow a path while it is recording a video. Some keyframes are extracted from the video. The extracted keyframes are called visual path and the interval between each two keyframes is called a segment. Later, the robot uses these keyframes to navigate autonomously to follow the desired path. Funnel lane is a recent method to follow visual paths which was proposed by Chen and Birchfield. The method requires a single camera with no calibration or any further calculations such as Jacobian, homography or fundamental matrix. A qualitative comparison between features coordinates is done to follow the visual path. Although experimental results on ground and flying robots show the effectiveness of this method, the method has some limitations. It cannot deal with all types of turning conditions such as rotations in place. Another limitation is an ambiguity between translation and rotation which in some cases may cause the robot to deviate from the desired path. In this paper, we introduce the sloped funnel lane and we explain how it can overcome these limitations. In addition, some challenging scenarios were conducted on a real ground robot to show that. Also, the accuracy and the repeatability of both methods were compared in two different paths. The results show that sloped funnel lane is superior.

**Index Terms**—visual path, qualitative visual navigation, funnel lane, sloped funnel lane, robot navigation.

## I. INTRODUCTION

THE process of determining a safe and appropriate path from a starting point to a goal point is called navigation. There are variant methods which use different sensors to perform it. Recently, visual navigation methods have been considered by the researchers due to the development of powerful processing modules and the expansion of their applications in mobile robots. These methods are used in both ground [4], [5], [6], [9], [10], [15], [20], [21] and flying [11], [12], [13], [14], [19] autonomous robots.

Regardless of the kind of robots, the visual navigation methods can be categorized into two types [1]: map-based and map-less visual navigation.

Map-based visual navigation methods [18], [20], [21] are based on extracting a model of the environment where the robot has to find its location on it.

Mohamad Mahdi Kassir was with the Artificial Intelligence Laboratory, Department of Electrical and Computer Engineering, Isfahan University of Technology, Isfahan, Iran. e-mail: m.kaseer@ec.iut.ac.ir

Maziar Palhang was with the Artificial Intelligence Laboratory, Department of Electrical and Computer Engineering, Isfahan University of Technology, Isfahan, Iran. e-mail: palhang@cc.iut.ac.ir.

Mohammad Reza Ahamadzadeh, Department of Electrical and Computer Engineering, Isfahan University of Technology, Isfahan, Iran. e-mail: ahamadzadeh@cc.iut.ac.ir.

Map-less visual navigation methods [16], [17], [22] do not need such a model to navigate in the environment. The robot depends on the elements observed in the environment to navigate.

Some navigation methods display the environment with sequential images which characterize the desired path. They are considered as map-less visual navigation methods that are based on visual teach and repeat technique. The main advantages of these methods are scalability, not needing global metric map construction, and simple implementation. The images can be gathered easily from an environment. These methods can have more applications especially for robots with limited memory.

On the other hand, according to the lack of scale and geometric information, following such paths is not easy.

In this paper, our navigation system falls into the category of visual teach and repeat technique. In the teaching phase, the robot is guided to follow a path while recording a video, after that keyframes are extracted from the recorded video to make the visual path. The intervals between two consecutive keyframes are called segments.

In the repeating phase, the robot has to be able to localize its segment and to follow the visual path autonomously. Usually, a method is used to control the robot inside a segment in the visual path and a criterion is defined to switch from a segment to the next segment until reaching the last keyframe. Visual servoing is a well-known technique which is used to control the robot inside a segment. Visual servoing approaches usually need calculations such as Jacobian [3] and homography or fundamental matrix [10], [11], [12].

Another approach is the funnel lane that was proposed by Chen and Birchfield [5]. The robot follows the path by making qualitative comparisons between the features in the teaching phase and the repeating phase. The method does not require any calculation to relate world coordinates to image coordinates or to relate the coordinates between images. Funnel lane assumes that the optical axis of the attached camera is parallel to the heading direction of the robot. A region is determined based on two constraints of each feature. This region is called the funnel lane. The robot tries to move inside this region. Funnel lane has been implemented on ground robot [5] and on quadrotor [2], [14], [24].

Standard funnel lane theory has some limitations. It gives no information about the type of turning which prevents the robot from dealing with some turning conditions such as rotation in place. Another limitation is the ambiguity between translation and rotation which happens when the obtained funnel lane is not narrow enough which can cause the robot to deviate from

the desired path.

In this paper, we introduce **sloped funnel lane** which tries to overcome these limitations. A third constraint is considered by looking at all features together. Two slopes are defined based on this constraint which is used to determine the type of turning and to reduce the ambiguity. Experimental results show the success of this approach.

In the rest of this paper, first, some notations and assumptions are introduced which are used throughout the paper. After that, the method to create the visual path will be discussed. In section IV, we have a brief discussion about the funnel lane concept and its limitations. Then we will explain the sloped funnel lane which is proposed in this paper and we show how the sloped funnel lane overcomes the limitations of the standard funnel lane. After that, experimental examples that show how the proposed sloped funnel lane successfully follows a visual path in which the standard funnel lane failed to follow, is presented. Finally, we will have a conclusion.

## II. NOTATIONS AND ASSUMPTIONS

In visual navigation systems some assumptions must be considered: enough light exist in the environment, the scene is often static, the environment contains enough texture to extract enough features, there is sufficient overlap between frames and the change of the conditions in the teaching phase and repeating phase does not affect the feature matching process in the repeating phase very much.

Some notations are used in this paper as follows:

- $V_i$  is the video taken from path  $i$ .
- $KF_{i,j}$  is the keyframe number  $j$  in path  $i$ .
- $KFs_i$  is all keyframes in path  $i$ .
- $S_{i,j}$  is the segment  $j$  in path  $i$ ,  $S_{i,j} : j \in \{1, 2, ..n - 1\}$ .
- $F_a$  features of image  $a$ .
- $RF_a$  right features of image  $a$ .
- $LF_a$  left features of image  $a$ .
- $MF(a, b)$  matched features of image  $a$  with image  $b$ .
- $NMF(a, b)$  is the number of matched features of image  $a$  with image  $b$ .
- $\sigma_a$  is the standard deviation of  $x$  coordinates features in image  $a$ .
- $StdRatio(a, b)$  is the ratio of standard deviation of  $x$  coordinates of  $MF(a, b)$  to the standard deviation of  $x$  coordinates of  $MF(b, a)$ .
- $ED(a, b)$  is the Euclidean distance between the median of  $x$  coordinates of  $MF(a, b)$  and the median of  $x$  coordinates of  $MF(b, a)$ .

Where figure 1 shows a video recorded from a path consisting  $m$  frames,  $n$  keyframes are selected from it and segment  $i - 1$  as shown in the figure is the interval between keyframe  $i - 1$  and keyframe  $i$ .

## III. VISUAL PATH CREATING

A robot is controlled to follow a path manually while it is recording a video. Some keyframes are selected from the video. The selected keyframes are called **visual path**. To select these keyframes, features of the first frame are detected and tracked in the video. A keyframe is selected when the

percentage of successfully tracked features falls below 50 percent. The process is repeated until reaching the end of the video.

The successfully tracked features in each segment are stored with their coordinates because they are used in the repeating phase.

## IV. STANDARD FUNNEL LANE

Standard funnel lane concept was introduced by Chen and Birchfield [5]. The robot is controlled such that it is able to reach a destination image according to the image it receives from its attached camera. The camera optical axis is parallel to the robot heading and its optical axis passes through the axis of rotation of the robot. First, we have a review on standard funnel lane. Then the motion control based on it will be explained.

Suppose that the robot wants to move from current location to location  $KF_{i,j}$ . There are some fixed landmarks that are seen in the camera of the robot in both locations as shown in figure 2. Suppose we have both current image and the destination keyframe image and the origin of the feature's coordinates is at the intersection of the optical axis and the image plane. If the robot goes forward in a straight line with the same heading direction as that of  $KF_{i,j}$ , the point  $u^c$  will move away from the origin of the feature's coordinates toward  $u^j$ , when the robot reaches the destination point  $u^c$  will reach  $u^j$ .

**Definition 1:** A funnel lane of a fixed landmark  $L$  and a robot location  $KF_{i,j}$  is the set of locations  $FL_{L,KF_{i,j}}$  such that, for each  $C \in FL_{L,KF_{i,j}}$ , the two funnel constraints are satisfied:

$$|u^c| < |u^j| \quad (1)$$

$$\text{sign}(u^c) = \text{sign}(u^j) \quad (2)$$

where  $u^c$  and  $u^j$  are the coordinates of the image projection of  $L$  at locations  $C$  and  $KF_{i,j}$ , respectively.

If the robot is on the path toward keyframe  $j$  with the same heading direction, then two constraints are satisfied. As shown in figure 3a, if the constraints are satisfied then the robot lies within a region called the funnel lane. If the heading direction of the robot is not the same direction of keyframe  $j$ , the lines of the funnel lane are rotated by an angle depending on the angle that the robot has with destination keyframe  $j$  as shown in figure 3b.

Each feature must satisfy two constraints and so for each feature we have a funnel lane region created. By intersecting all funnel lanes, a final funnel lane is obtained which satisfies all of the feature constraints. Figure 4 shows an example of how the final funnel lane will be if we have two features.

### A. Motion control based on standard funnel lane

The robot continually moves forward while it is inside the funnel lane, when the robot goes outside the funnel lane from the right side it gets left command and when the robot goes outside the funnel lane from the left side it gets a right command to keep it in the funnel lane.

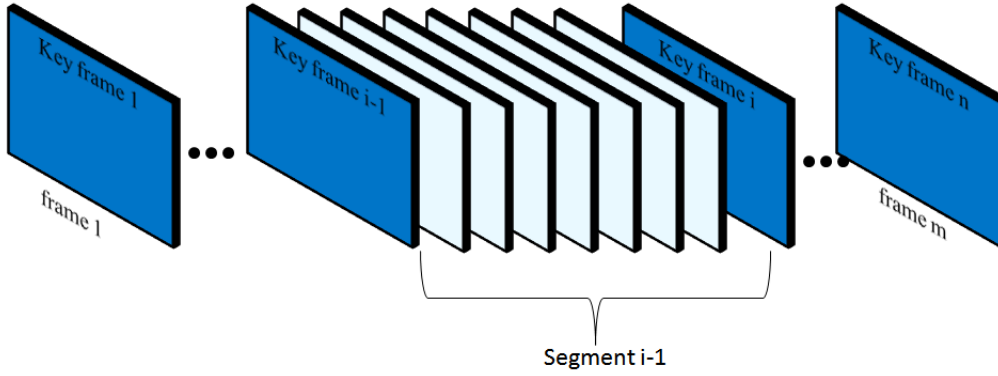


Fig. 1:  $N$  keyframes are selected from  $m$  frames to create a visual path and segment  $i - 1$  as shown is the interval between keyframe  $i - 1$  and keyframe  $i$

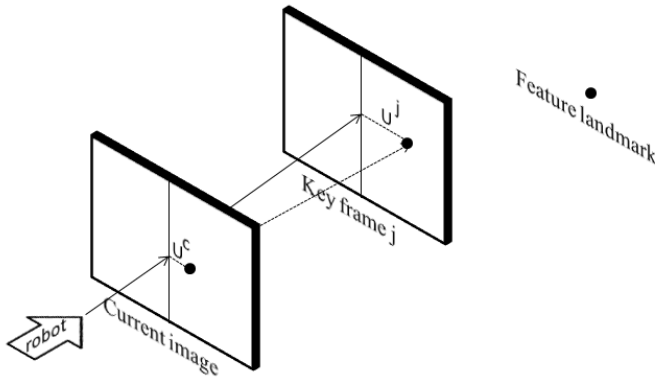


Fig. 2: A robot is moving on straight line with a camera attached on it which the optical axis is parallel to the robot heading.

### B. Limitations

Motion control based on standard funnel lane has some limitations, which as explained in the following:

#### 1- Undefined type of turning:

Motion control based on funnel lane is actually a bang-bang control. The robot is moving forward and it turns by an amount to the right or to the left depending on the command it gets[5]. The Standard funnel lane gives no information about the type of turning whether it is wide, sharp or rotation in place. In motion control based on funnel lane, the driving and the turning speed are set before the repeating phase and are not changed along the path, adaptively. Due to this limitation, the robot is not able to deal with all turning conditions such as rotation in place [13] and it cannot correct its direction easily when it deviates from the desired path especially in turnings.

#### 2- Ambiguity of translation and rotation:

In the standard funnel lane, there is an ambiguity between translation (going straight) and rotation (turning) inside the funnel lane itself [5]. This ambiguity shows itself mainly when the final funnel lane created is not narrow enough. To make it more clear consider figure 5 where there are features just in the right side and the  $x$  coordinates of the destination features

lay on the right side of the current features. In the first case, a turning causes the destination features lay on the right side of the current features (figure 5a). In the second case the path is straightforward and therefore the destination features lay on the right side of the current features (figure 5b). In the standard funnel lane, the two constraints are satisfied and the robot falls on the funnel lane, which means it will get a straightforward command. This causes the robot to deviate from the path if destination features laid on the right of the current features was from a rotation.

If there were features on the left side, the left features could help to reduce this problem. This explains why in standard funnel lane the matched features must appear in both sides. Furthermore, existing features on both sides of the image does not always resolve the ambiguity and the obtained funnel lane may remain wide. The features far from the center of the image create wide funnel lanes. Unfortunately, it is not guaranteed that the matched features lay on both sides and being near the center of the image. In turning conditions the remaining features will be sometimes shifted to one side. This problem also happens when the robot has deviated from the path. Even existing features on both sides of the image and near the center does not prevent from occurring this ambiguity because of losing features due to tracking failure or moving objects.

### V. SLOPED FUNNEL LANE

Sloped funnel lane is an extended method of standard funnel lane. First, we will explain the sloped funnel lane. Then the motion control based on it will be described. After that, we will show how the sloped funnel lane can overcome the limitations of the standard funnel lane.

The standard funnel lane gives no information about the type of turning and there is an ambiguity between translation and rotation as explained. Standard funnel lane is created according to the fact that the features will move away from the center of the feature's coordinates toward the edge of the images.

Actually, standard funnel lane is created based on two constraints and it considers each feature individually. Another constraint can be considered by looking at all features together according to the fact that the features will move away from each other as the robot moves forward. So we can conclude

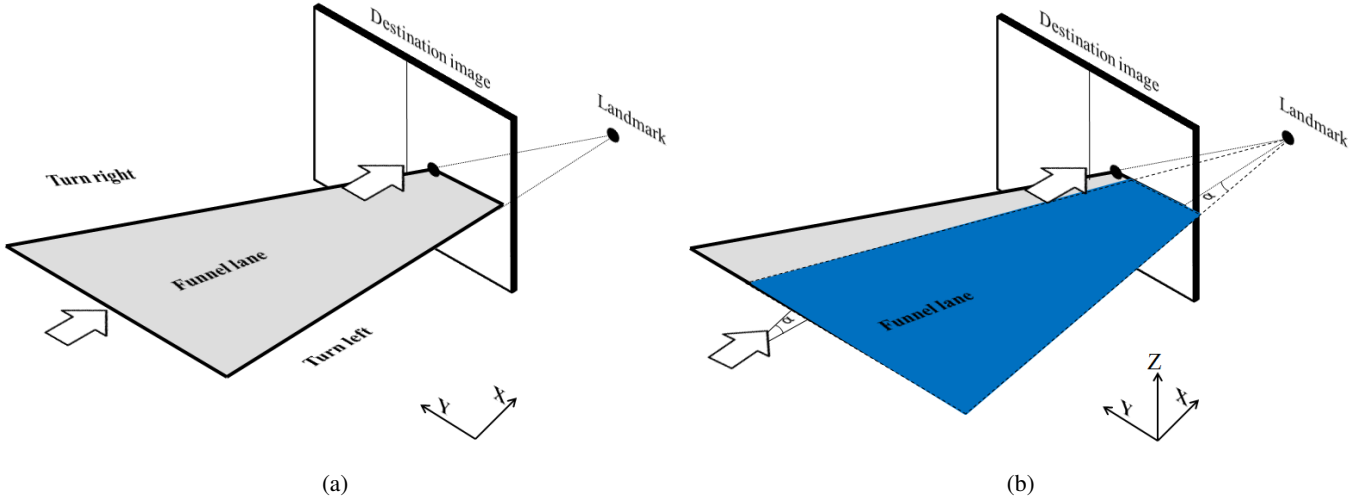


Fig. 3: (a) Funnel lane created when the robot has the same heading angle with the destination, (b) Funnel lane created when the robot has a heading angle  $\alpha$  with the destination

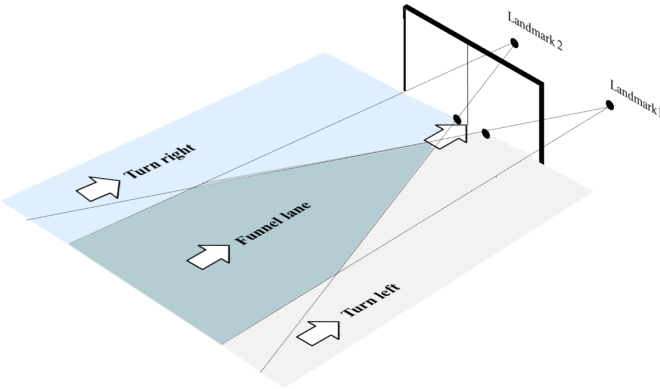


Fig. 4: Final funnel lane created by two features when the robot has the same heading angle with the destination

that the ratio of the standard deviation of  $x$  coordinates of all matched features in the current image to the standard deviation of  $x$  coordinates of their correspondence in destination image will become larger as the robot moves forward toward the destination. In other words, the standard deviation of the destination  $KF_{i,j}$  is larger than the standard deviation of the current image if the destination keyframe is ahead of the current image.

To take the third constraint into account we add slopes to the standard funnel lane. The idea is inspired by the movement of a ball on a sloped surface. If the surface has a slope toward front, the ball moves forward. If the surface has a slope toward left or right sides the ball will roll to the left or right. Moreover, if the surface has a slope toward front and left /right side at the same time the ball will roll forward and tend to the left /right. Depending on the amount of the slope toward forward and toward left or right the ball will roll in different trajectories. In our case, the ball is the robot and the surface is the sloped funnel lane. To define such a surface we define the slope around  $y$  axis inversely proportional to the

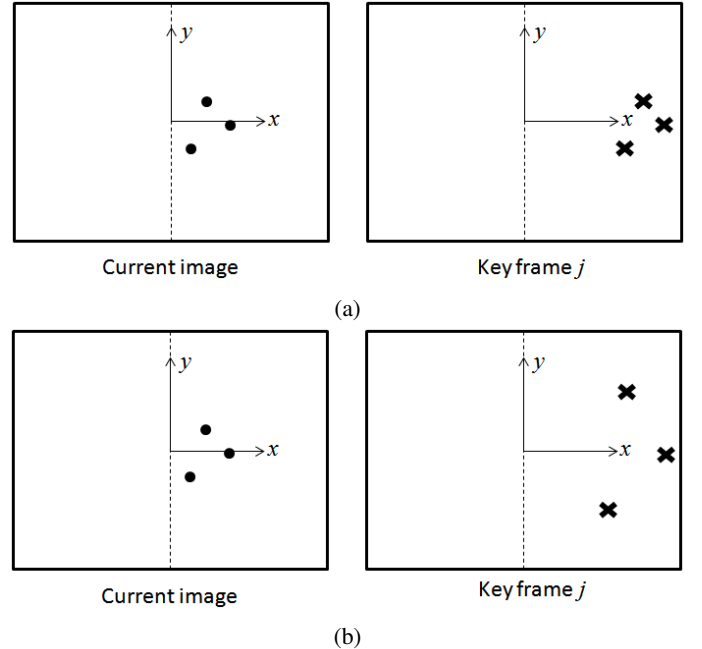


Fig. 5: Circle symbols show the positions of the current features and star symbols show the positions of their corresponding features in destination keyframe  $j$ . (a) A left turning causes the destination features to lay on the right side of the current features, (b) A forward movement causes the destination features to lay on the right side of the current features

ratio of the standard deviation  $StdRatio(c, KF_{i,j})$  and the slope around  $x$  axis is defined proportional to the difference of current and destination feature coordinates. Therefore, we define the sloped funnel lane as follows:

**Definition 2:** A sloped funnel lane of a fixed landmark  $L$  and a robot location  $(KF_{i,j})$  is the set of locations  $SFL_{L, KF_{i,j}}$  such that, for each  $C \in SFL_{L, KF_{i,j}}$ , the following three

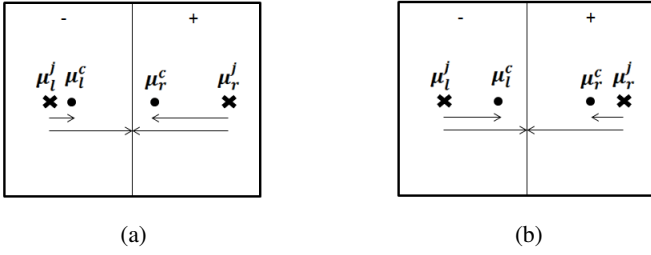


Fig. 6: Two examples of summing the slope of both sloped funnel lanes representing each side: (a) the sum will be positive, (b) the sum will be negative.

funnel constraints are satisfied:

$$|u^c| < |u^j| \quad (3)$$

$$\text{sign}(u^c) = \text{sign}(u^j) \quad (4)$$

$$\sigma^c / \sigma^j < 1 \quad (5)$$

And the funnel lane slope around  $y$  axis is  $\beta \times (1 - (\sigma^c / \sigma^{KF_{i,j}}))$  and the slope around  $x$  axis is  $\gamma \times (u^j - u^c) / |u^j|$ , where  $u^c$  and  $u^j$  are the coordinates of the image projection of  $L$  at the locations  $C$  and  $KF_{i,j}$ , respectively.  $\sigma^c$  and  $\sigma^{KF_{i,j}}$  are the standard deviation of the features coordinates at locations  $C$  and  $KF_{i,j}$ , respectively.

Figure 7a shows a sloped funnel lane with slope around  $x$  axis and figure 7b shows a sloped funnel lane with slope around  $y$  axis.

The sloped funnel lane as the standard funnel lane if the heading direction of the robot is not the same direction with the destination keyframe  $j$ , the lines of the funnel lane are rotated by an angle depending on the angle that the robot has with the destination keyframe  $j$ .

Instead of creating a sloped funnel lane for each feature to form the final sloped funnel lane as in standard funnel lane, the final sloped funnel lane is formed just by two sloped funnel lanes. One of them represents the right features (median of right features  $\mu_r$ ) and the other one represents the left features (median of left features  $\mu_l$ ). The features of the current image are considered right or left features according to being on the right or left side of the destination keyframe. The sloped funnel lane which represents the right or left features is a sloped funnel lane created by the median of the right or left features.

A method is needed to combine two sloped funnel lanes that represent each side. When there is no feature to represent one side, the final funnel lane is the same as the other funnel lane. Otherwise the final sloped funnel lane will be the intersection of both standard funnel lanes with slope around  $y$  axis is  $\beta \times (1 - (\sigma^c / \sigma^{KF_{i,j}}))$  (note that the standard deviation of both right and left features is considered) and the slope around  $x$  axis is obtained by summing their slopes around  $x$  axis which is  $\gamma \times (\mu_l^j - \mu_l^c) / |\mu_l^j| + (\mu_r^j - \mu_r^c) / |\mu_r^j|$ . Figure 6 shows an example of summing these two slopes. The sum of two slopes in figure 6a will be positive and in figure 6b will be negative. Figure 7d shows the obtained sloped funnel lane when the robot heading angle is the same as the destination keyframe

with a slope around  $y$  axis and no slope around  $x$  axis. Figure 7c demonstrates with the same conditions but with just a slope around  $x$  axis.

#### A. Motion control based on sloped funnel lane

The robot moves forward until it is inside a funnel lane with no slope around  $x$  axis. When the funnel lane has a positive slope around  $x$  axis greater than a specific threshold, the robot gets a left command depending on the slope around  $y$  axis and when it has a negative slope lower than a specific threshold, it gets a right command depending on the slope around  $y$  axis. In other words, the slope around  $x$  axis determines whether the robot has to turn or not and the slope around  $y$  axis determines the type of turning. If there is no slope around  $x$  axis the robot moves straight forward no matter of the slope around  $y$  axis is. Having same  $x$  slope, the less the  $y$  slope, the sharper the robot turns and vice versa. As the slope around  $y$  axis gets near zero, the turning command will be more like rotation in place. When the robot goes outside the sloped funnel lane from the right side it gets a left command and when the robot goes outside the sloped funnel lane from the left side it gets a right command depending on the slope around  $y$  axis to keep it in the funnel lane.

#### B. How sloped funnel lane overcomes limitations of standard funnel lane

The sloped funnel lane can deal with the limitations that are mentioned in section IV-B. Adding another constraint which is based on all features together can help to solve these limitations. We will demonstrate the limitations and explain how sloped funnel lane can handle them.

##### 1-Undefined type of turning

The type of turning is defined in sloped funnel lane. As we explained, the slope around  $x$  axis determines whether the robot has to turn or not, and the slope around  $y$  axis determines the kind of turning. For example, in a rotation in place conditions, the slope around  $y$  axis will be near zero which means that the sloped funnel lane can recognize it and send the appropriate command. In addition, if the robot deviates from the path especially in turnings, it can correct its direction by decreasing its translation speed and increasing rotation.

##### 2-Ambiguity of translation and rotation

As mentioned before, in the standard funnel lane an ambiguity in the funnel lane itself exists. In the sloped funnel lane, the ambiguity of rotation and the translation is resolved by adding the third constraint. In sloped funnel lane, even when the robot is in the sloped funnel lane, it is not free to move forward and its movement is determined by the slope around the  $x$  axis. Also, large funnel lane is not an important issue in sloped funnel lane. For example, in figure 5, the standard funnel lane does not distinguish between both keyframes as we have shown before, but the sloped funnel lane distinguishes between them because the slope around  $y$  axis is different.

The reason is that the slope around  $y$  axis is inversely proportional to the standard deviation ratio which in the first case is closer to 1 than the second case. In both cases, a left

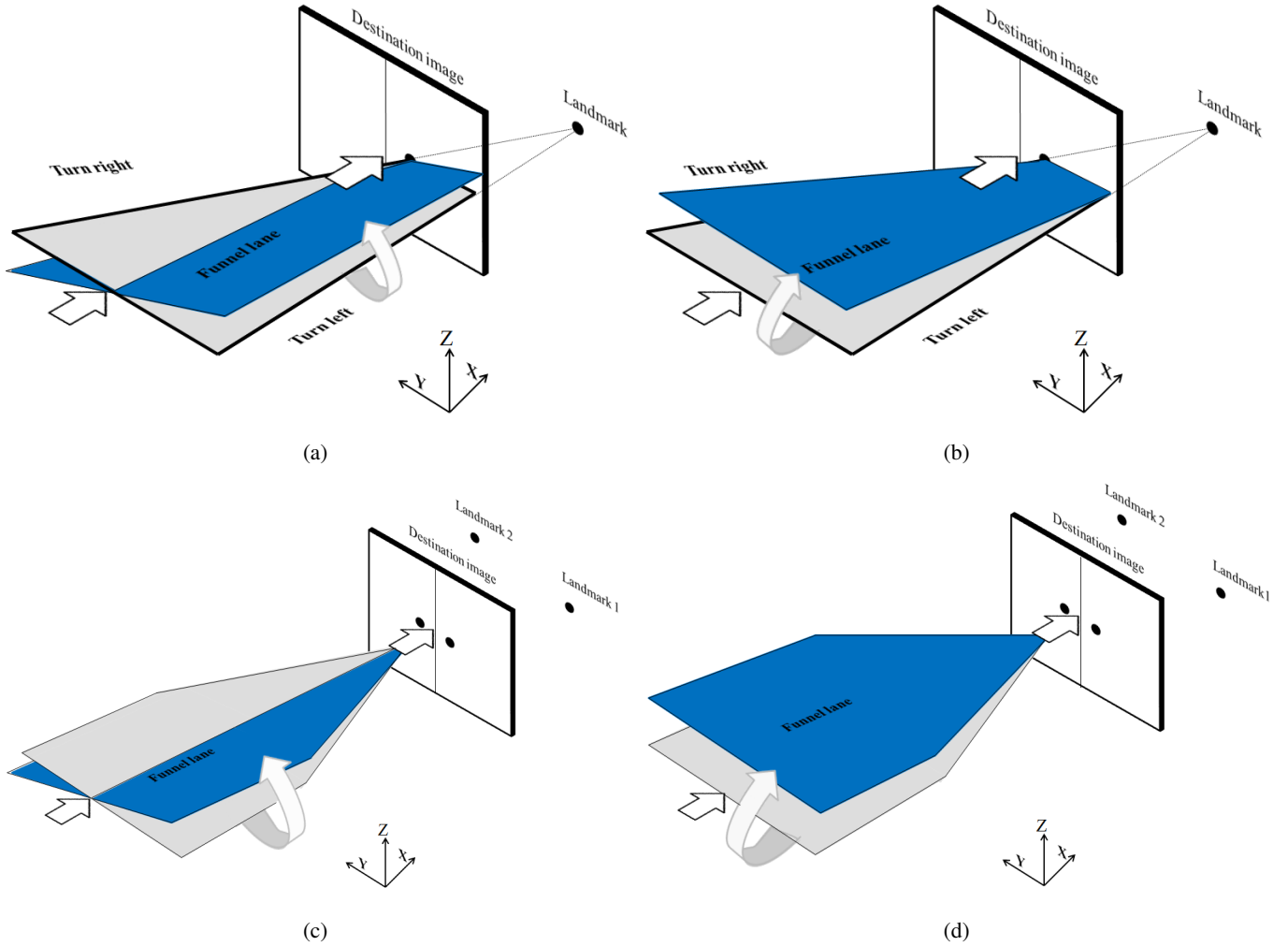


Fig. 7: (a) Sloped funnel lane with slope around  $y$  axis, (b) Sloped funnel lane with slope around  $x$  axis, (c) Final sloped funnel lane created by two features with slope around  $y$  axis, (d) final sloped funnel lane created by two features with slope around  $x$  axis

command is sent. Therefore no funnel lane is created for the right features and slope around  $x$  axis will be positive. But in the first case, the robot turns sharper, and in the second case a turning near to moving straight forward occurs.

## VI. KEYFRAME SWITCHING CRITERION

Funnel lane is a method to control a robot between two keyframes and how to move inside a segment. An important issue is how to define the criterion to switch to another keyframe. Mean square error between the coordinates of current features and features in the destination keyframe can be used as a criterion. Z. Chen and S. T. Birchfield [6] proposed a method based on MSE. In their method, switching happens when MSE increases. It supposed that the MSE error will become smaller as the robot moves toward the destination image, and the error is decreasing until reaching it. Actually, in our experiments, the error was not decreasing due to insensitive steering. A lot of switching happens because the criterion needs a very sensitive steering and steering a little more than necessary or even losing some features cause the

MSE not to decrease. Another method [5] uses mean square error with odometry information to define a probability for switching. In [13] the switching criterion is based on comparing RANSAC 2 points and RANSAC 5 points. This method needs RANSAC calculation which is time-consuming. Another method is based on matching two successive keyframes [2]. Therefore a matching is required for every cycle to know when to switch.

In our work, a method based on the third constraint defined in the sloped funnel lane is used. When  $StdRatio(currentimage, destinationkeyframe)$  becomes greater than 1 and the Euclidean distance of the median of both coordinates  $ED(currentimage, destinationkeyframe)$  becomes less than a threshold, a switching happens.

## VII. EXPERIMENTAL RESULTS

Real experiments were conducted on a robot with a VEX platform [23]. The robot uses an IP camera and sends the images  $320 \times 200$  using WIFI to the laptop. Blob features are used in this paper. A well-known blob detection technique



Fig. 8: The robot is used to evaluate the proposed navigation method

is SIFT [8] that uses the difference of Gaussian operator to detect features. SURF [7] is a speeded-up version of SIFT. It approximates the Gaussian with a box filter and the convolution with a box filter can be calculated simultaneously for different scales. In our experiments, we choose SURF detectors to speed up the navigation algorithm and its length is chosen to be 64. Larger length gives more accuracy but it decreases the speed of features matching. For feature tracking KanadeLucasTomasi (KLT) algorithm with default block size [31 31] is used. The algorithm is executed on a laptop and the commands are sent to the robot for path following. The algorithm is implemented in MATLAB 2016 on a VAIO laptop (core i7 1.73GHz). The robot is shown in figure 8. First, the robot is controlled manually from the laptop while recording a video from the traversed path. After that, the visual path is constructed as explained in the previous sections. Then, the robot is placed on the same initial point and is controlled by the algorithm running on the laptop to follow the recorded visual path.

The method used for visual navigation after creating the visual path is presented in algorithm 1.

In section V-B we explained how sloped funnel lane outperforms standard funnel lane. In this section, we compare the two methods in six practical scenarios. Moreover, two paths are chosen to compare the accuracy and the repeatability of our method with the standard funnel lane.

First, the visual path is created. Then the robot is placed at the initial point and it tries to follow the visual path once with the sloped funnel lane and again with the standard funnel lane. Figure 9 shows the features in the current image and the features matched with them in the destination keyframe. Also  $StdRatio(c, KF_{i,1})$  is shown at the top of the figure.

#### A. Six practical scenarios

The goal is to evaluate the path following ability of both algorithms in six challenging scenarios. Three scenarios are

#### Algorithm 1 visual navigation

```

1: assumed: The visual path  $i$  consists from  $n$  keyframes
2:  $C$ =capture the current image
3:  $j=1$ 
4: Detect surf features of  $C$ 
5: Match features of  $C$  with  $KF_{i,j}$ 
6:  $switch = false$ 
7:  $NoF = NMF(C, KF_{i,j})$ 
8: while  $j < n$  do
9:   if  $StdRatio(C, KF_{i,j+1}) > 1$  and
      $ED(C, KF_{i,j+1}) < Threshold$  or  $switch = true$ 
     then  $\triangleright$  A switching to the next segment is happens
10:     $j = j + 1$ 
11:     $C$ =capture the current image
12:    Detect surf features of  $C$ 
13:    Match features of  $C$  with  $KF_{i,j}$ 
14:     $NoF = NMF(C, KF_{i,j})$ 
15:  else  $\triangleright$  Control inside a segment
16:    if  $NoF > Threshold$  then  $\triangleright$  Sufficient
     features remained
17:      Track the matched features with KLT
18:       $NoF = NoF - lost\ features$ 
19:      Control the robot with the sloped funnel lane
20:    else
21:      while  $NoF < Threshold$  do
22:         $C$ =capture the current image
23:        Detect surf features of  $C$ 
24:        Match features of  $C$  with  $KF_{i,j}$ 
25:         $NoF = NMF(C, KF_{i,j})$ 
26:        Stop the robot
27:      end while
28:    end if
29:  end if
30: end while

```



(a)

Fig. 9: The matched features of the current image with the destination keyframe is shown by green color and their corresponding destination features are shown by red color,  $StdRatio(\text{current image, destination keyframe})$  is shown at the top of the figure

TABLE I: The comparison of the accuracy and the repeatability of both standard funnel lane and sloped funnel lane

	standard funnel lane acc. / rep.	sloped funnel lane acc. / rep.
<b>Indoor with sharp turn</b>	3.45 / 0.55	<b>1.31 / 0.51</b>
<b>Indoor almost straight</b>	1.19 / 0.62	<b>1.0 / 0.46</b>

indoor and the rest are outdoor. Two of the three chosen indoor scenarios are short and challenging, while the other one is almost a straight path. The first one is a 9-meter path inside a room with narrow space. First, the robot is controlled to follow the path after that the robot is placed at the same initial point. In the first trial, the robot follows the path with the standard funnel lane and in the second trial, it follows the path with sloped funnel lane. Figure 10a shows the teaching path and both paths followed by the robot with the standard and sloped funnel lane. The robot was not able to follow the path by standard funnel lane and it hits the chair. The reason is that the type of turning is undefined in the standard funnel lane and the robot turns by a constant speed. A small deviation from the desired path or switching later than it should, make it impossible to correct its direction especially in such a scenario with narrow space.

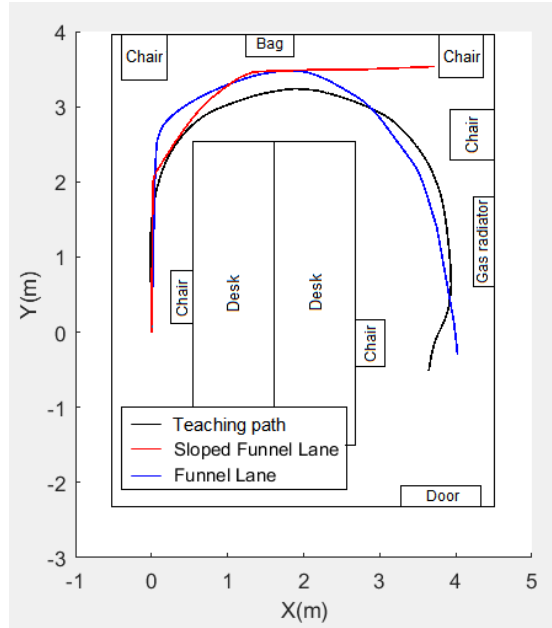
The second scenario is another 6-meter path with one turning to the left and with wide space. The robot in the repeating phase is placed two meters in front of the initial point in the teaching phase. Figure 10b shows the followed paths with both methods. Even though in the standard funnel lane the robot constantly gets left commands, it is not able to follow the path because it is placed two meters in front of the initial point. The sloped funnel lane was able to correct its direction because it gets a sharper turning command to get back on the desired path.

The third indoor path is almost straight 25 meters in a corridor as shown in 10c. The results were very close and both methods followed the path successfully.

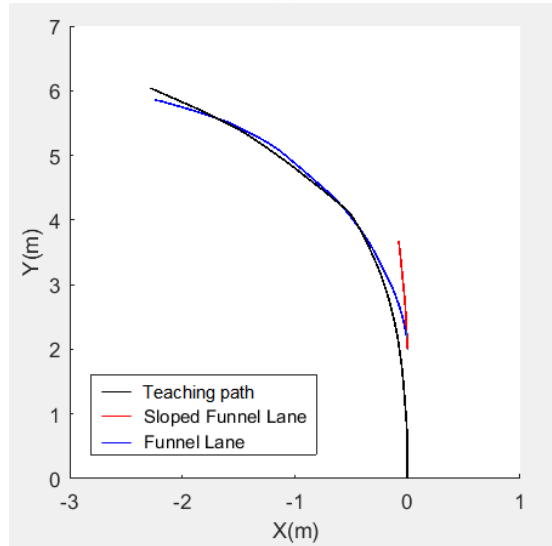
We have chosen three outdoor scenarios. The first one is a parking lot. The robot is controlled to park between two cars near each other as shown in 11a. Both methods get perform equally well. But in standard funnel lane the robot corrects its direction hardly and it gets closer to the side of the car which increases failure risk. Another outdoor scenario is a closed loop path with a dynamic situation. In the teaching phase the robot is controlled to follow a looped path, and in the repeating phase two of the parked cars are left and the ability to follow the path with both methods is checked. Figure 11b shows the results of both methods. The gray cars are the ones left in the repeating phase. The robot failed to follow the path by standard funnel lane because a lot of features of one side were lost which causes a wide funnel lane and ambiguity between translation and rotation. Last outdoor scenario is a path with wide turning and as shown in figure 11c both methods follow the path successfully.

### B. Accuracy and repeatability comparison

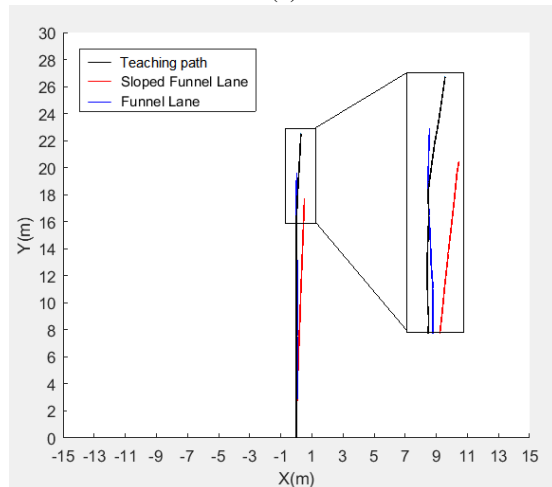
The six practical scenarios showed the ability of both methods to follow some challenging paths. In this section, we



(a)



(b)



(c)

Fig. 10: (a) The first indoor scenario with narrow space (b)The second scenario with a different initial point at the repeating phase and (c) The third indoor scenario with an almost straight path.



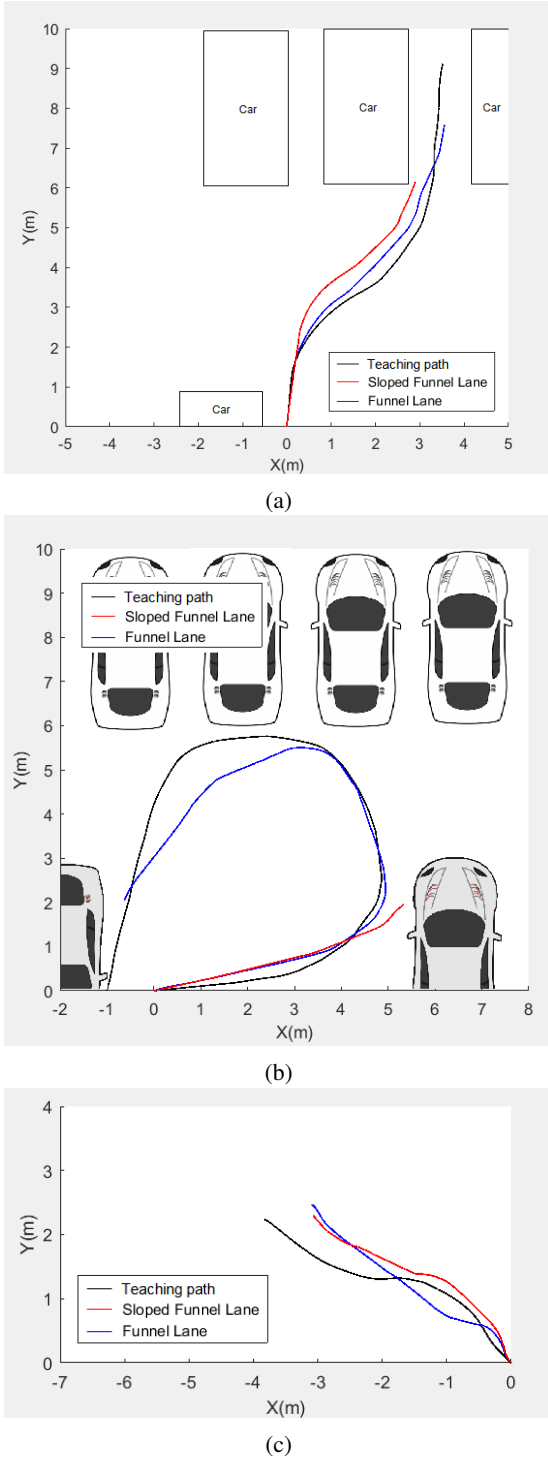


Fig. 11: (a) The first outdoor parking scenario (b) The second outdoor scenario is a closed loop that two cars are left in the repeating phase and (c) The third outdoor scenario with wide turning.



Fig. 12: The keyframes selected to create the visual path which standard funnel lane fails to follow and sloped funnel lane follows successfully.

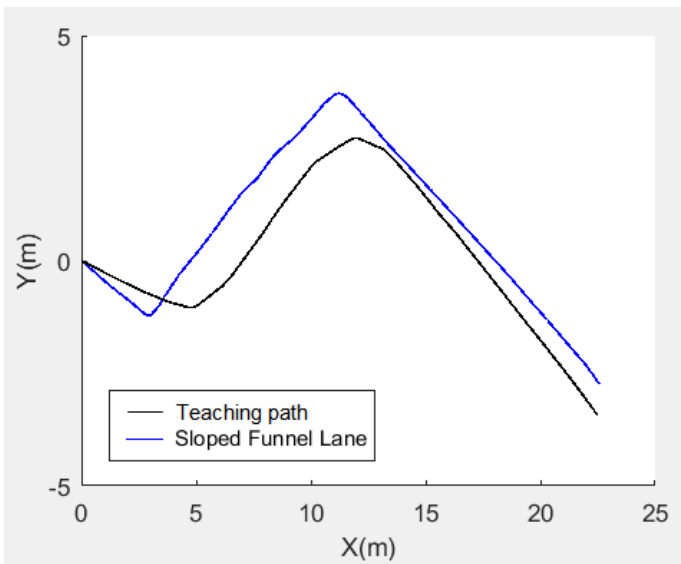
compare the accuracy and the repeatability of both methods. Two indoor paths are chosen and the experience was repeated for ten times by both algorithms. The first one is a 10-meter path with one sharp turn to the left and low texture indoor environment. Figure 12 shows the selected keyframes that create the visual path of the route. The second one is a 10 meter indoor almost straight route. The distance between the final point reached by the robot and the desired final point is calculated. The average RMS Euclidean distance and the standard deviation which expresses the accuracy and the repeatability of the algorithms are shown in table I.

Actually, the robot fails to follow the path in the sharp turn with the standard funnel lane. The reason is that in this turning the remaining features in the image are shifted to one side which causes the standard funnel lane to fail, while the sloped funnel lane was able to follow the path successfully in most cases.

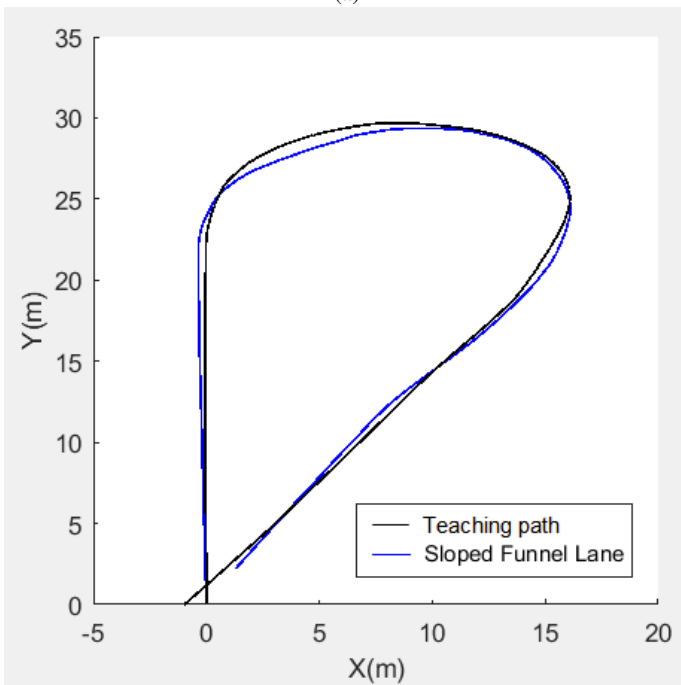
It is noteworthy that sloped funnel lane is as good as standard funnel lane and the experiments performed shows the deficiencies of standard funnel lane has been able to successfully solve. Two additional experiments are conducted to demonstrate the effectiveness of the approach. The first one is a 30-meter indoor path inside the department and the second one is a 70-meter outdoor path inside IUT campus. Figure 13a and figure 13b show the results. The most important thing in experiments is to consider the assumptions mentioned in section II.

## VIII. CONCLUSION

In this paper, a qualitative visual navigation based on sloped funnel lane concept was proposed. In the teaching phase, the robot is controlled manually to follow a path. In the repeating



(a)



(b)

Fig. 13: (a) The indoor path and (b) the outdoor path, the sloped funnel lane follows them successfully.

phase, the robot has to follow the desired path autonomously. First, a visual path was created by selecting some keyframes from the video taken by the robot in the teaching phase. After that in the repeating phase, the concept of the sloped funnel lane which overcomes some limitations of the standard funnel lane was introduced. The proposed sloped funnel lane, unlike the standard funnel lane, can deal with different turning conditions including rotation in place. As well it reduces the ambiguity of translation and rotation which may occur in the standard funnel lane. As a result, a more robust and reliable method than the standard funnel lane has been proposed.

The limitations of the standard funnel lane were explained in details and we demonstrated how our proposed sloped funnel lane overcomes them. Moreover, some experiments were conducted on a real robot and the results showed that our proposed method outperforms the standard funnel lane.

#### ACKNOWLEDGMENT

The authors would like to thank Artificial Intelligence laboratory members for their support.

#### REFERENCES

- [1] F. Bonin-Font, A. Ortiz, and G. Oliver, Visual Navigation for Mobile Robots: A Survey, *J. Intell. Robot. Syst.*, 2008.
- [2] T. Nguyen, G. K. I. Mann, R. G. Gosine, and A. Vardy, Appearance-Based Visual-Teach-And-Repeat Navigation Technique for Micro Aerial Vehicle, *J. Intell. Robot. Syst. Theory Appl.*, 2016.
- [3] D. Burschka and G. Hager, Vision-based Control of Mobile Robots, in *Proc. IEEE Int. Conf. Robot. Autom.*, 2001.
- [4] A. Diosi, A. Remazeilles, S. egvi, and F. Chaumette, Experimental evaluation of an urban visual path following framework, in *IFAC Proceedings Volumes (IFAC-PapersOnline)*, 2007.
- [5] Z. Chen and S. T. Birchfield, Qualitative vision-based path following, *IEEE Trans. Robot.*, 2009.
- [6] C. Zhichao and S. T. Birchfield, Qualitative vision-based mobile robot navigation, in *Proceedings - IEEE International Conference on Robotics and Automation*, 2006.
- [7] H. Bay, A. Ess, T. Tuytelaars, and L. Van Gool, Speeded-Up Robust Features (SURF), *Comput. Vis. Image Underst.*, 2008.
- [8] D. G. Lowe, Distinctive image features from scale-invariant keypoints, *Int. J. Comput. Vis.*, 2004.
- [9] J. J. Guerrero, R. Martinez-Cantin, and C. Sags, Visual map-less navigation based on homographies, *J. Robot. Syst.*, 2005.
- [10] B. L. B. Liang and N. Pears, Visual navigation using planar homographies, *Proc. 2002 IEEE Int. Conf. Robot. Autom. (Cat. No.02CH37292)*, 2002.
- [11] A. Remazeilles and F. Chaumette, Image-based robot navigation from an image memory, *Rob. Auton. Syst.*, 2007.
- [12] S. egvi, A. Remazeilles, A. Diosi, and F. Chaumette, Large scale vision-based navigation without an accurate global reconstruction, in *Proceedings of the IEEE Computer Society Conference on Computer Vision and Pattern Recognition*, 2007.
- [13] Tien Do, Luis C. Carrillo-arce, Stergios I. Roumeliotis, "Autonomous Flights through Image-defined Paths", *International Symposium of Robotics Research (ISRR)*, 2015.
- [14] T. Nguyen, G. K. I. Mann, and R. G. Gosine, Vision-based qualitative path-following control of quadrotor aerial vehicle, in *2014 International Conference on Unmanned Aircraft Systems, ICUAS 2014 - Conference Proceedings*, 2014.
- [15] E. Royer, M. Lhuillier, M. Dhome, and J.-M. Lavest, Monocular Vision for Mobile Robot Localization and Autonomous Navigation, *Int. J. Comput. Vis.*, 2007.
- [16] H. Chao, Y. Gu, and J. Gross, A comparative study of optical flow and traditional sensors in UAV navigation, *Am. Control*, 2013.
- [17] M. V. Srinivasan, Honeybees as a Model for the Study of Visually Guided Flight, *Navigation, and Biologically Inspired Robotics*, *Physiol. Rev.*, 2011.
- [18] K. Kidono, J. Miura, and Y. Shirai, Autonomous visual navigation of a mobile robot using a human-guided experience, in *Robotics and Autonomous Systems*, 2002.
- [19] E. Royer, J. Bom, M. Dhome, B. Thuilot, M. Lhuillier, and F. Marmoton, Outdoor autonomous navigation using monocular vision, *Proc. IEEE/RSJ Int. Conf. Intell. Robot. Syst.*, 2005.
- [20] A. Remazeilles, F. Chaumette, and P. Gros, 3D Navigation Based on a Visual Memory, in *International Conference on Robotics and Automation*, 2006.
- [21] Y. Matsumoto, K. Ikeda, M. Inaba, and H. Inoue, Visual navigation using omnidirectional view sequence, in *Proceedings 1999 IEEE/RSJ International Conference on Intelligent Robots and Systems. Human and Environment Friendly Robots with High Intelligence and Emotional Quotients (Cat. No.99CH36289)*, 1999.

- [22] H. Chao, Y. Gu, and M. Napolitano, A survey of optical flow techniques for UAV navigation applications, in 2013 International Conference on Unmanned Aircraft Systems, ICUAS 2013 - Conference Proceedings, 2013.
- [23] [http : //www.vexrobotics.comvisitedin2018](http://www.vexrobotics.comvisitedin2018).
- [24] A. G. Toudeshki, F. Shamshirdar, and R.Vaughan, UAV Visual Teach and Repeat Using Only Semantic Object Features, CoRR, 2018.

PLACE  
PHOTO  
HERE

**Mohamad Mahdi kassir** received his B.S. degree in Information technology Engineering from Isfahan University of technology, Iran, in 2011 and the Master degree in Artificial Intelligence from Isfahan University of Technology, in 2013. He works in Artificial Intelligence laboratory since 2012. Currently, he is a Ph.D. student of Artificial Intelligence in Isfahan University of Technology. His current research interests include robotics and computer vision.

PLACE  
PHOTO  
HERE

**Maziar Palhang** received his B.Sc. in Computer Hardware from Sharif University of Technology, Tehran, Iran. He received his M.Comp.Sc. and Ph.D. from the University of New South Wales, Sydney, Australia. He was a Postdoctoral fellow in UNSW as well. He later joined Electrical and Computer Engineering Department of Isfahan University of Technology, Isfahan, Iran. He has been the Chairman of Humanoid league of IranOpen Competitions. His research interests are Machine Learning, Computer Vision, and Robotics.

PLACE  
PHOTO  
HERE

**Mohammad Reza Ahmadzadeh** received his B.Sc. degree in Electronic Engineering from the Ferdowsi University of Mashhad, Iran in 1989 and the M.Sc. degree in Electronic Engineering from the University of Tarbiat Modarres, Tehran in 1992. He received his Ph.D. from University of Surrey, UK in 2001. He was a lecturer at Shiraz University from 1993-1997, and an Assistant Professor from 2001-2004. He is an Associate Professor of Electrical Engineering at Isfahan University of Technology, Iran from 2004. His research interests include reasoning with uncertainty,

pattern recognition, image processing, expert systems, information fusion and neural networks.